Annals of Botany **111**: 905–915, 2013
doi:10.1093/aob/mct061, available online at www.aob.oxfordjournals.org

ANNALS OF BOTANY
Founded 1887

Diurnal pattern of stomatal conductance in the large-leaved temperate liana *Aristolochia macrophylla* depends on spatial position within the leaf lamina

Tatiana Miranda[1], Martin Ebner[1], Christopher Traiser[2] and Anita Roth-Nebelsick[2,*]

[1]*Department of Geosciences, University of Tübingen, Sigwartstr. 10, D-72076 Tübingen, Germany and*
[2]*State Museum of Natural History, Rosenstein 1, D-70191 Stuttgart, Germany*
** For correspondence. E-mail anita.rothnebelsick@smns-bw.de*

Received: 20 November 2012 Revision requested: 9 January 2013 Accepted: 29 January 2013

• *Background and Aims* The large distance between peripheral leaf regions and the petiole in large leaves is expected to cause stronger negative water potentials at the leaf apex and marginal zones compared with more central or basal leaf regions. Leaf zone-specific differences in water supply and/or gas exchange may therefore be anticipated. In this study, an investigation was made to see whether zonal differences in gas exchange regulation can be detected in large leaves.
• *Methods* The diurnal course of stomatal conductance, g_s, was monitored at defined lamina zones during two consecutive vegetation periods in the liana *Aristolochia macrophylla* that has large leaves. Local climate and stem water potential were also monitored to include parameters involved in stomatal response. Additionally, leaf zonal vein densities were measured to assess possible trends in local hydraulic supply.
• *Key Results* It was found that the diurnal pattern of g_s depends on the position within a leaf in *A. macrophylla*. The highest values during the early morning were shown by the apical region, with subsequent decline later in the morning and a further gradual decline towards the evening. The diurnal pattern of g_s at the marginal regions was similar to that of the leaf tip but showed a time lag of about 1 h. At the leaf base, the diurnal pattern of g_s was similar to that of the margins but with lower maximum g_s. At the the leaf centre regions, g_s tended to show quite constant moderate values during most of the day. Densities of minor veins were lower at the margin and tip compared with the centre and base.
• *Conclusions* Gas exchange regulation appears to be zone specific in *A. macrophylla* leaves. It is suggested that the spatial–diurnal pattern of g_s expressed by *A. macrophylla* leaves represents a strategy to prevent leaf zonal water stress and subsequent vein embolism.

Key words: Stomatal conductance, heterogeneous stomatal conductance, macrophyll, leaf size, leaf venation, diurnal pattern, stem water potential, *Aristolochia macrophylla*.

INTRODUCTION

Plant gas exchange is regulated by a sophisticated control of stomatal conductance, g_s, that responds to various environmental stimuli, particularly light, vapour pressure deficit (VPD), the water supply situation at the roots, mediated by abscisic acid (ABA), and the internal CO_2 concentration (Wong *et al.*, 1979; Buckley, 2005). All these responses to various stimuli are integrated into a system of regulation of g_s to prevent transpiration rates that would lead to excessive embolism of stem and leaves (Sperry *et al.*, 2002; Brodribb *et al.*, 2003; Sack and Holbrook, 2006), while simultaneously allowing for harvesting as much carbon as possible. One manifestation of co-ordinating these two conflicting tasks is the typical diurnal pattern of g_s, with the highest g_s values during the morning when the VPD is low and subsequent decline of g_s during the day under increasing VPD (Larcher, 2003). This diurnal pattern is in accordance with the strategy of maximizing carbon gain while minimizing water loss (Cowan and Farquhar, 1977; Berninger *et al.*, 1996; Katul *et al.*, 2010). Instantaneous g_s can vary considerably among leaves of an individual plant, depending on the actual environmental conditions experienced by single leaves, and can be additionally modulated according to the position within a crown (Sellin and Kupper, 2005).

Many models of stomatal conductance are based on the assumption of instantaneous g_s being uniform over a leaf (Ball *et al.*, 1987; Collatz *et al.*, 1991; Leuning, 1995; Dewar, 2002; Damour *et al.*, 2010; Katul *et al.*, 2010). There is, however, ample evidence that g_s varies substantially within single leaves (Terashima, 1992). There are various types of stomatal heterogeneity. Local variances in stomatal density (SD) and size can be involved, but the main reason for non-uniform stomatal conductance is heterogeneous stomatal aperture. During the last few years, attention was mainly focused on 'stomatal patchiness', the phenomenon of joint behaviour of groups of stomata (patches). The degree of aperture of one stomatal patch is independent from the aperture of adjacent patches, and complex patterns of g_s over a leaf may result (Pospíšilová and Šantrůček, 1994; Mott and Buckley, 2000). There are, however, also macroscopic differences in g_s (Terashima, 1992). Nardini *et al.* (2008) found for

tobacco leaves that g_s was higher in the apical region than in the basal parts of the leaf. In leaves of *Commelina communis*, a gradient in g_s between the central and the peripheral parts of the leaves was detected (Smith *et al.*, 1989). The reasons for the various types of stomatal heterogeneity are still under debate. In the case of stomatal patchiness, problems with short-term responses to environmental perturbations are assumed to play a role (Buckley, 2005; Kaiser, 2009). For the macroscopic gradients found in *C. communis* and *Nicotiana tabacum*, hydraulic factors have been suggested that lead to spatial variations in water supply over the leaf lamina, making local adaptations of gas exchange necessary (Smith *et al.*, 1989; Nardini *et al.*, 2008).

In large leaves, a considerable amount of the leaf area will be quite distant from the point of insertion of the petiole that represents the source of water for the lamina. The risk of water stress at peripheral leaf regions is particularly enhanced if g_s is high and homogeneous over the whole lamina. Under these circumstances, the leaf water potential (ψ_{leaf}) should show minimum values along the margins and the tip (Roth-Nebelsick *et al.*, 2001; Cochard *et al.*, 2004). Moreover, differences in local boundary layer structure may arise in large leaves, with the lowest boundary layer thickness at peripheral regions. For a large and entire leaf, the margins and tip should therefore be more prone to water stress than basal or more central leaf regions since these sites are located at the 'end' of the pressure drop that extends over the leaf venation during transpiration. In fact, size is one leaf trait that shows significant negative correlation with decreasing humidity (Givnish, 1987; Scoffoni *et al.*, 2011).

Spatial differences in stomatal regulation mitigating or preventing leaf zonal water stress might therefore be anticipated. Since, however, instantaneous g_s at any point within a leaf is the result of superposition of various factors to which stomata respond (diurnal patterns, response to external environmental stimuli, local water status or signals from the roots), g_s is prone to a high statistical noise that may obscure such zonal patterns. In the study presented here, g_s was monitored for defined leaf zones in the large-leaved temperate deciduous vine *Aristolochia macrophylla* over two consecutive vegetation periods. *Aristolochia macrophylla* shows a dense crown with large, thin and entire leaves. Furthermore, the leaves of *A. macrophylla* show almost identical length and width. This shape leads to a high 'accumulation' of leaf area that should particularly promote two-dimensional gradients of water supply. Along with g_s, xylem water potential and climate parameters were also monitored. The study was performed on an adult specimen under natural conditions.

MATERIALS AND METHODS

Study site and plant material

The study was conducted on a specimen of *A. macrophylla* growing in the Arboretum at the Botanical Garden of the University of Tübingen. The location of the specimen is 48 ° 32′26·16″N, 9°2′2·56″E, 412 m a.s.l. The soil at the growing site is situated above an argillaceous parent rock material of the late Triassic formation, which promotes a favourable water supply. The plant grows entwined around a dead tree and reached a height of around 6 m at the time of the study (Supplementary Data Fig. S1). The growing site of the specimen is fully exposed to sunlight. The leaves considered were at a height of 1·50–1·90 m above ground, and showed an area of 29 086 + 5928 mm^2. The leaves therefore belong to the macrophyll category (Ellis *et al.*, 2009).

Climate parameters

The climatic parameters at the study site were recorded by the mobile weather station WD-2700 (Watchdog, PCE group, PCE Germany, Meschede, Germany). The recordings were read with the software WD-SPEC. Air temperature, soil humidity, leaf temperature, air humidity, photosynthetic active radiation (PAR) and solar radiation, precipitation, wind speed and wind direction were logged at intervals of 5 min during the entire observation period. The VPD was calculated from relative air humidity, air temperature and the equation for saturated vapour pressure according to Jones (1992). Soil water potential was measured regularly during the study period by using the tensiometer device of the Watchdog weather station.

Stem water potential

Xylem water potential in the stem (ψ_{xylem}) was monitored continuously at regular intervals during the growing seasons of 2010 (May–August) and 2011 (June–July). ψ_{xylem} was measured *in situ* by using the stem psychrometer StepLog (Plant Water Status Instruments, Guelph, Ontario, Canada) (Dixon and Tyree, 1984). The measurement intervals were selected according to the weather conditions. During rainy periods, no measurements were carried out. The sensor was attached to the base of the stem, at a height of about 30 cm. The bark was removed carefully until sapwood with an area similar to the contact area of the sensor, about 27 mm^2, was exposed (Vogt, 2001). The sensor was then fixed to the sapwood by clamps and tape, sealed with silica gel, and carefully isolated using foam material. Mounting of the StepLog was finished by wrapping plastic film around the stem and sensor. Furthermore, the sensor was always attached at a site on the stem that was shielded by leaves from insolation. Measurements were performed with a time interval of 60 min.

The position of the sensor had to be changed every 2 weeks and the open sapwood was sealed with a special paste after the sensor was removed. This long-term monitoring was possible since the plant, due to its size, shows a ramifying stem whose numerous distal branches were large enough to allow for these manipulations. Before each measurement, the sensor was calibrated with 0·1, 0·3, 0·5, 0·7 and 0·9 molal (mol kg^{-1}) NaCl solutions at 20 °C (Lang, 1967). With each solution, six values were taken at 15 min intervals. The mean of the last four values was estimated for a calibration line. To account for thermal gradients, the values of the first 5 h after installation were discarded.

Stomatal conductance

The value of g_s was measured with a Porometer AP4 (Delta-T Devices Ltd, Cambridge, UK) at different and defined positions or zones within the leaf lamina (= leaf

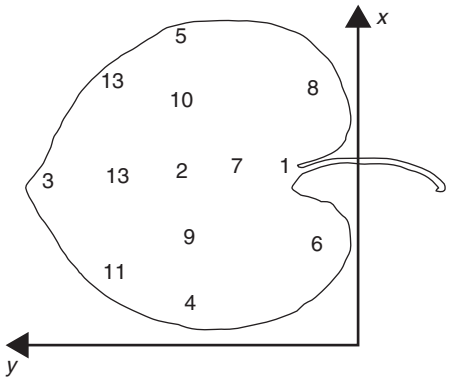

FIG. 1. The various leaf zones that were monitored with respect to the diurnal pattern of g_s.

zones, indicated in Fig. 1). The contact area between the leaf and measurement chamber is 51 mm^2 (17 mm × 3 mm). Measurements were taken at these positions over entire days at each hour during the vegetation periods 2010 and 2011, simultaneously with the monitoring of ψ_{xylem}. Measurements were taken on at least four leaves at each hourly measurement. Since measurements were taken under very different daytime conditions (high humidity and cooler temperatures early in the morning, lower humidity and higher temperatures during noon/afternoon), we had to recalibrate the porometer several times over a day, necessary after each adaption of the relative humidity set point in the measurement cup to air humidity. According to pilot studies at the study site, we waited until a stable value appeared, usually after about 7–10 s. This was necessary because the early morning measurements in particular were difficult to perform due to the high air humidity and we wanted to perform all measurements in a similar way.

In order to avoid permanent damage of the leaf tissue inflicted by repeated attachment of the measurement chamber of the porometer, a different set of randomly selected leaves was used for each measurement. A total of about 4000 single measurements were taken on about 40 d during the entire study. The number of measurements at the various leaf zones are: zone 1, $n = 521$; zone 2, $n = 394$; zone 3, $n = 573$; zone 4, $n = 554$; zone 5, $n = 545$; zone 6, $n = 336$; zone 7, $n = 74$; zone 8, $n = 301$; zone 9, $n = 126$; zone 10, $n = 126$; zone 11, $n = 105$; zone 12, $n = 345$; and zone 13, $n = 99$. To assess local insolation at the leaves, we used the radiation data which are provided by the light sensor of the porometer during g_s measurement.

Leaf osmotic potential

Osmotic potential, ψ_{osm}, was measured by using a portable PSYPRO water potential system (Wescor Inc., Logan, UT, USA). As osmotic potential sensor, a C-52 sample chamber (Wescor Inc.), was connected to the PSYPRO. Measurement of ψ_{osm} also included leaves which were used for determination of g_s. Leaf sap was obtained by using the Markhart leaf press (Wescor Inc.) which allows for extraction of the liquid sample directly onto a filter paper disc. After soaking the filter paper disc, it was immediately transferred to the C-52 sample chamber.

Measurements were performed partially on-site or in the laboratory. In the latter case, leaves were harvested in the field, sealed in a plastic bag and immediately brought to the laboratory where they were frozen at −20 °C while still sealed in the bag. Liquid samples were then obtained after thawing. Previous control measurements on liquid samples obtained from frozen vs. non-frozen leaves revealed no significant differences in osmotic potential. The measurement and calibration routines of the PSYPRO water potential system was carried out according to standard methods with commercial calibration solutions of different osmotic potential (Wescor Inc.). Calibration was performed before the measurements.

Stomatal density

Stomatal density was determined for the leaf zones 1–5 (Fig. 1) by using scanning electron microscopy (SEM), with a LEO Model 1450 VP (Variable Pressure) (LEO Electron Microscopy Ltd, Cambridge, UK) available at the Institute for Geosciences, University of Tübingen. For SEM, dry material was used. After mounting on stubs, the leaf pieces were sputtered with gold, with a BAL-TEC Model SCD 005/CEA 035 (BAL-TEC GmbH, Witten, Germany). The samples were observed under vacuum mode, with an accelerating voltage of 10 kV and a working distance of 15 mm. The SD (number of stomata per leaf area = number/mm^2) was counted in five adjacent areas of each zone 1–5 for a minimum area of 300 μm^2 for each single count (Poole and Kürschner, 1999).

Vein density

Since leaf hydraulic conductance correlates with venation density (Sack and Holbrook, 2006; Nardini *et al.*, 2008), the density of lower order (second and third order veins) and higher order (= minor) veins was measured at different leaf zones to assess possible regional differences in leaf hydraulic conductance. Digital images were taken from three randomly selected leaves of *A. macrophylla*. Leaf veins of first, second and third order were identified according to the 'Manual of leaf architecture' (Ellis *et al.*, 2009). Determination of vein density was performed by using ImageJ, Version 1.46 (Rasband, 1997–2012). Four identical rectangular sample areas of 20 × 30 mm were located at the top, central, basal and marginal parts of the lamina (Supplementary Data Fig. S2). In order to calculate the vein density (mm mm^{-2}) of lower order veins, the veins were then digitalized by polylines within the sample areas. The sum of vein length within each sample area was determined for the second and third vein order separately.

Higher order vein density was obtained by measuring the total length of minor veins within a partial area of the sample areas that were also considered for lower order vein density. These measurements were conducted for the same three leaves. For this, stereomicroscope images of the lower leaf side of *A. macrophylla* were sufficient since the minor veins are dark green and therefore clearly visible within the lighter green lamina. The total minor vein length of images of leaf areas of about 50–100 mm^2 was determined by using ImageJ, Version 1·46, (Rasband, 1997–2012). All minor veins were outlined by using the line tool, and the total length of the lines was measured.

Hydraulic conductivity at different positions of the major vein

To assess trends in local hydraulic conductivity along the major vein, conduit number and size were also determined at leaf zones 1–3 for the three leaves that were considered for vein density measurements. Hand sections were prepared using the fresh material. Sections through the major vein at leaf zones 1, 2 and 3 were then identified. The cross-sectional shape of the conduits was mostly elliptic and the lengths of both the major and minor axis were determined by using the line tool of ImageJ. The sections also allowed the number of conduits within the major vein at the three different leaf zones to be determined.

According to the Hagen–Poiseuille law for elliptic tubes, the relationship between volume flow rate Q, pressure gradient ($\Delta p/\Delta l$) and conduit size is as follows:

$$Q = \frac{\pi}{4\mu} \times \frac{a^3 b^3}{a^2 + b^2} \times \frac{\Delta p}{\Delta l} \quad (1)$$

with μ = viscosity of water ($1{\cdot}003\ 10^{-3}$ Pa s at 20 °C), a = half-length of the long axis of the ellipse, b = half-length of the short axis of the ellipse, p = pressure and l = tube length (Bruus, 2008).

For a bundle of capillaries, hydraulic conductivity K_h can be calculated (N = number of conduits; Leyton, 1975):

$$K_h = N\left[\frac{\pi}{4\mu} \times \frac{a^3 b^3}{a^2 + b^2}\right] \quad (2)$$

K_h from eqn (2) should indicate the maximum potential local hydraulic conductivity of the vein as limited by conduit size and number. For calculation of an approximative value of K_h, mean values of a and b were used. It should be noted that an exact calculation of K_h requires the determination of the efficient conduit size parameters, a_{eff} and b_{eff}, which are somewhat larger than a_{mean} and b_{mean} (Leyton, 1975).

Statistical analysis

For the statistical analysis, SPSS 19 (IBM, USA) and Past (Hammer *et al.*, 2001) were used. To test the differences between zonal g_s values for statistical significance, the non-parametric Kruskal–Wallis test for independent samples was applied with subsequent Mann–Whitney test plus Bonferroni correction, because the data (according to the Shapiro test) showed no clear trend for normal distribution. g_s was tested for significant differences between leaf zones at different intervals during the daytime. These intervals were defined as 'early morning' (EM), 0500–0800 h; 'morning' (M), from after 0800 h to 1100 h; 'noon' (N), from after 1100 h to 1400 h; 'early afternoon' (EA), from after 1400 h to 1600 h; 'afternoon' (A), from after 1600h to 1900 h; and 'evening' (E), later than 1900 h.

The graphical representation of the zonal distribution of g_s was created by applying the 'Interpolation tool' of 'Matlab' (TheMathWorks, Inc.). For each of the 13 considered regions, the zonal mean values of g_s were derived for the defined time intervals and used as a basis for the interpolation maps representing the distribution of g_s over the whole lamina at each time interval.

For the stomatal density, SD, no clear trend for normal distribution was found, and the Kruskal–Wallis test was also used in this case.

RESULTS

Climate parameters

Daily climate at the measurement site, averaged over the time period of measurement, is shown in Fig. 2. VPD increases rapidly during a day, reaching a maximum around early afternoon, parallel to the increase of air temperature that attains an average maximum of about 25 °C at noon. For the rest of the day, neither parameter changed substantially until early evening.

Stem water potential

The mean temporal pattern of ψ_{xylem} for the entire measurement period is shown in Fig. 3. In the early morning, ψ_{xylem} is about −0·2 MPa, and starts to decline rapidly after 0900 h, reaching its daily minimum of about −1·5 MPa at 1200 h. In the afternoon, ψ_{xylem} starts to rise again. Pre-dawn values are reached during the night, at about 0300–0400 h. ψ_{xylem} is strongly correlated with VPD (Spearman's $\rho = 0{\cdot}663$, $P < 0{\cdot}001$, $n = 3674$).

Stomatal conductance

Figure 4 shows the diurnal course of $g_{s,mean}$, the mean of all measurements of g_s that were taken during a certain daytime

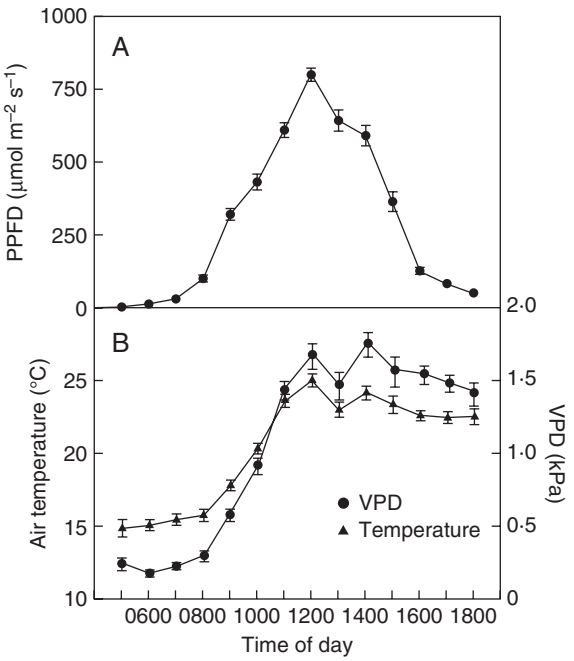

FIG. 2. Climate at the growing site of the *A. macrophylla* individual. The data were collected over the whole study period that comprised the vegetation periods 2010 and 2011. The mean values are plotted against hour of the day, with the error bars representing the 95 % confidence interval. (A) Photosynthetic photon flux density (PPFD). (B) Vapour pressure deficit (VPD) and air temperature, as indicated.

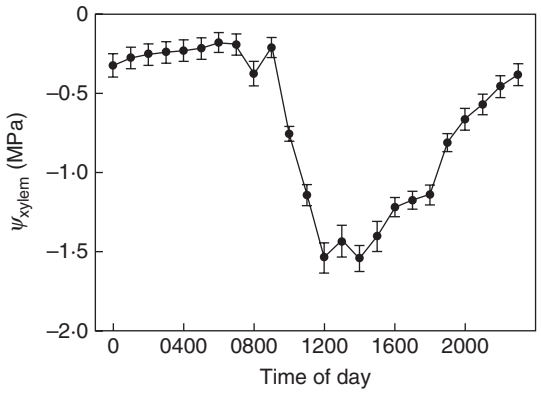

FIG. 3. Daily course of ψ_{xylem} within the stem of the *A. macrophylla* individual. The data were collected over the whole study period that comprised the vegetation periods 2010 and 2011. The mean values are plotted against hour of the day, with the error bars representing the 95 % confidence interval.

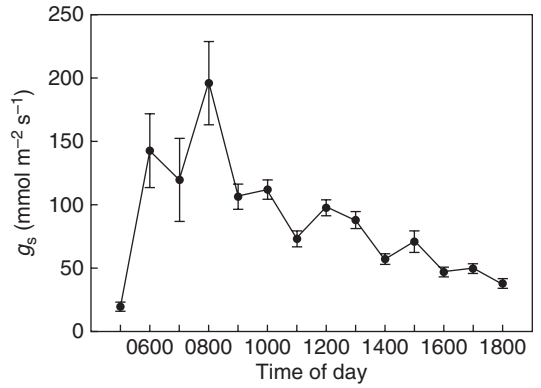

FIG. 4. Hourly mean values of g_s derived from all measurements during the study period. The error bars represent the 95 % confidence interval.

interval within the study period. $g_{s,mean}$ soars in the early morning, during dawn, and attains its maximum during the morning hours between 0800 and 0900 h. After this time, $g_{s,mean}$ decreases gradually, without any substantial rise for the rest of the day.

Spatial patterns of stomatal conductance

The diurnal pattern of g_s at the considered zones of the leaf lamina, $g_{s,zonal}$, is depicted in Fig. 5. There are distinct local differences visible for diurnal $g_{s,zonal}$. In the early morning (0500–800 h), $g_{s,zonal}$ is highest in the apical region of the leaf. Then, apical $g_{s,zonal}$ decreases and during the morning (0800–1100 h) is similar to the leaf margins, where $g_{s,zonal}$ is highest during the morning. During 'noon' (1100–1400 h), $g_{s,zonal}$ is substantially depressed over the whole lamina, with higher $g_{s,zonal}$ at the leaf base and the apical region. $g_{s,zonal}$ then decreases gradually during the rest of the day, with slightly higher values at the leaf tip and base than in the rest of the leaf. Central leaf regions show almost constantly low values. It should be noted that the contour maps shown in Fig. 5 do not contain any information on the areas between the measured zones. The 'true' g_s map may be more complex in reality (Lawson and Weyers, 1999). The complete data set of g_s is provided in Supplementary Data Fig. S3, showing a scatter plot of $g_{s,zonal}$ against time of day for each lamina zone (1–13).

Statistical tests were performed with respect to the significance of daytime differences in $g_{s,zonal}$ at the various lamina regions. The results for the early morning and morning are summarized in Table 1. Many differences between leaf regions that are visible in Fig. 5 are also statistically significant. For instance, early morning $g_{s,zonal}$ at the apical region is significantly different from that in most other regions. The original statistical tables are shown in Supplementary Data Table S1.

To assess a possible influence of local or temporal differences in irradiance on g_s, leaf zonal photosynthetic photon flux density (PPFD) was recorded simultaneously with $g_{s,zonal}$ during each measurement by the light sensor within the porometer cup. Figure 6 summarizes the diurnal course of $g_{s,zonal}$ and PPFD $_{zonal}$ for the lamina zones 1–5. These were selected because they showed the highest $g_{s,zonal}$ values throughout the measurements. Figure 6 shows that there are minor differences in PPFD for the various zones. The differences in the temporal course of $g_{s,zonal}$ appear, however, not to be caused by differences in the PPFD. Rather, $g_{s,zonal}$ follows a site-specific diurnal pattern. For example, at leaf zone 1, $g_{s,zonal}$ increases to its maximum value and then decreases substantially well before maximum irradiance is reached. The apical region shows a particularly strong and early increase in $g_{s,zonal}$ at dawn and holds this maximum for quite a long time, compared with the duration of the maximum $g_{s,zonal}$ at the other zones. $g_{s,zonal}$ decreases at all zones after 0900 h. A slight recovery is seen after 1100 h, but $g_{s,zonal}$ plunges again shortly afterwards with no substantial increase for the rest of the day. At all zones, $g_{s,zonal}$ reaches its maximum well before the PPFD maximum.

In Fig. 7 the diurnal courses of VPD, ψ_{xylem} and $g_{s,zonal}$ at three different leaf zones, the apical region (leaf zone 3) and two regions close to the leaf centre (leaf zones 9 and 10), are shown together. The central zones, which are situated opposite to each other across the major vein, show almost identical behaviour with respect to the diurnal $g_{s,zonal}$ pattern that differs greatly from the pattern at the tip during the morning, as expected from Fig. 5. $g_{s,zonal}$ at the leaf centre increases more slowly than at the tip and reaches much lower maximum values. The rapid decline at the leaf tip starts after a decrease in ψ_{xylem} and an increase in VPD set in. Shortly afterwards $g_{s,zonal}$ starts to drop at the tip, ψ_{xylem} shows a brief recovery towards the early morning value and then decreases continuously during the rest of the day.

Leaf osmotic potential

Mean ψ_{osm} data of leaf zones 1–4 and 5 (4 and 5 here summarized as 'margin') obtained during early morning and morning are shown in Fig. 8. According to the data, ψ_{osm} tends to be lower in the morning compared with the early morning. The lowest values occur at the leaf tip. Statistically significant differences between the data could, however, not be confirmed.

Stomatal density

Aristolochia macrophylla shows quite a low SD (Fig. 9). At the centre and the tip, higher values were found than at the

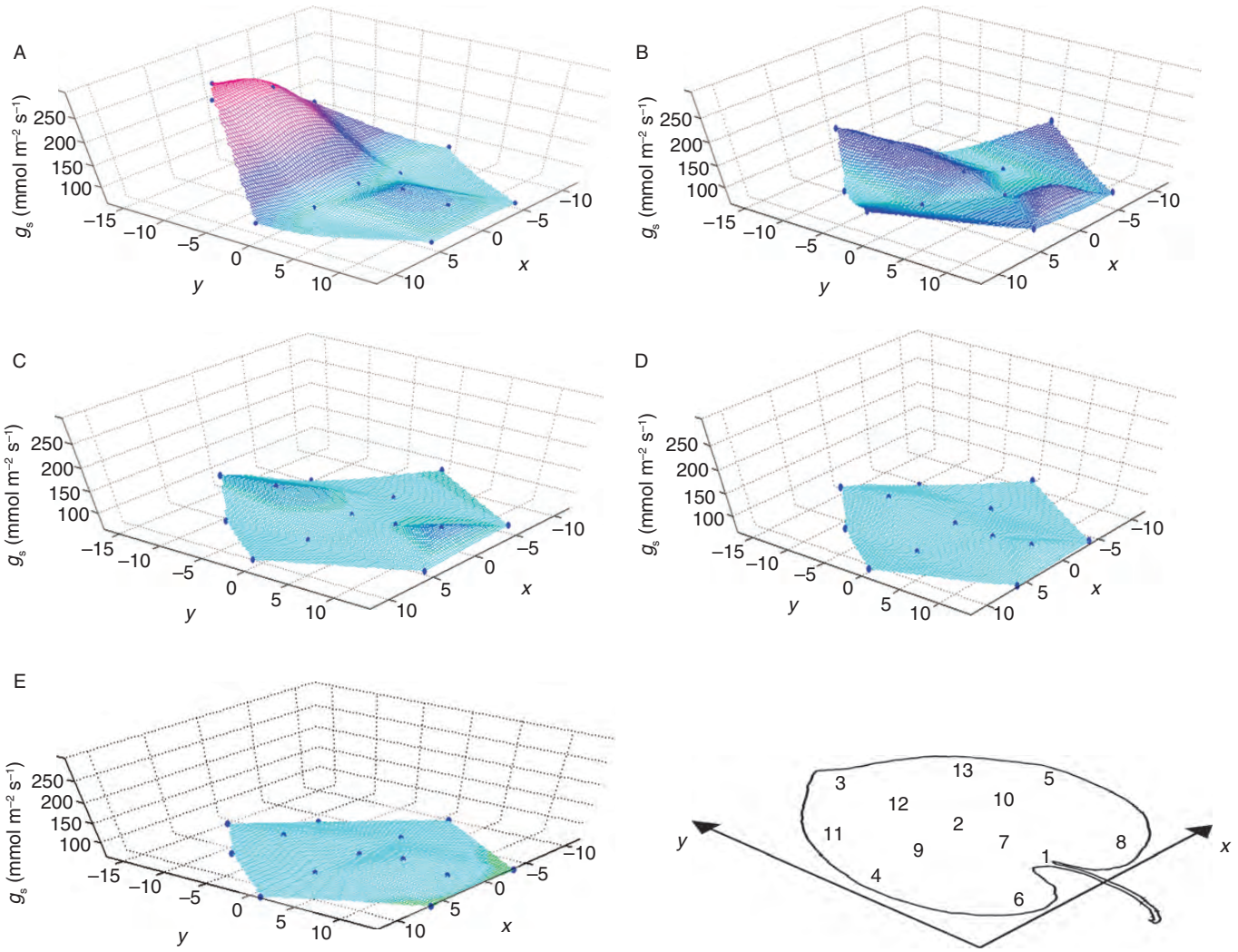

FIG. 5. Spatial representation of g_s of the various considered leaf zones at different times of the day over the study period. The points in the graphs indicate the leaf zones: an image showing the orientation of the graphs and the position markers with respect to the leaf is included. The graphs were generated by calculating the mean g_s within a certain time of day at the various zones, and then interpolating g_s at the zonal values with the Interpolation Tool of 'MatLab' for the entire lamina. The spatial co-ordinates of the *x*- and *y*-axis are relative co-ordinates to allow for showing the defined leaf zones. For example, (0,0) denotes the leaf centre, (0, −15) the uppermost point at the leaf tip, and (0, 15) the insertion point of the petiole. (A) 'Early morning' (EM), 0500–0800 h. (B) 'Morning' (M), from after 0800 h to1100 h. (C) 'Noon' (N), from after 1100 h to 1400 h. (D) 'Early afternoon' (EA), from after 1400 h to 1600 h. (E) 'Afternoon' (A), from after 1600 h to 1900 h.

margins and the leaf base. The differences between the tip and leaf centre and the other zones are statistically significant (Kruskal–Wallis, $P < 0{\cdot}001$, with subsequent Dunn's method of pairwise multiple comparison, $P < 0{\cdot}05$). We did not detect differences in stomatal size over the leaf.

Venation density and vein conduit size

The density of the lower order veins (second and third order) is plotted against leaf zones 1–4 and 5 in Fig. 10. The densities of both the second and the third order veins are highest at the base (leaf zone 1), lowest at the leaf centre (leaf zone 2) and then increase towards the leaf tip (leaf zone 3) and margin (leaf zones 4 and 5). Leaf zonal differences in venation densities are lower for the third order veins. Here, vein densities for leaf zones 3 and 4–5 are almost identical. For the third order veins, no statistically signficant differences between densities at the different leaf zones could be found. For the second order veins, however, analysis of variance (ANOVA) indicated statistically significant differences ($P = 0{\cdot}041$), with the Tukey test showing differences between leaf zones 1 and 2 ($P = 0{\cdot}035$). Minor vein density (vein order >3) at leaf zones 1–4 and 5 is also shown in Fig. 10. The density is lowest at the leaf tip and margins. The differences are statistically significant (ANOVA, $P = 0{\cdot}011$).

The results of conduit size and number within the major vein are summarized in Table 2. The long and short axes of the elliptically shaped cross-sections of the vein conduits are lowest at the tip. Additionally, the number of conduits within the major vein decreases, as expected. Correspondingly,

potential K_{vein}, as derived from the local dimensions of the conduits along the major vein, decreases, with a strong drop between the major vein centre and tip.

TABLE 1. *Statistical significance between differences in values of* g_s *at the considered leaf zones (see Fig. 1) during the early morning (0500–0800 h; indicated by *) and morning (from after 0800 h to 1100 h; indicated by †)*

Leaf zone	1	2	3	4	5	6	7	8	9	10	11	12	13
1													
2													
3	*	*											
4			*										
5			*										
6	†		*										
7													
8			*										
9	†		* †										
10													
11	†	†	†										
12	*	*		*	*	*		*	*	*	†		
13	†	†	†	†	†							†	

Statistical significance is marked if $P < 0{\cdot}05$ (Mann–Whitney tests after Bonferroni correction). The raw data can be found in Supplementary Data Table S1.

DISCUSSION

Leaf zonal g_s *and microclimate*

The daily courses of g_s are species-specific patterns resulting from the superposition of diurnal rhythm and responses to various environmental factors (Lösch *et al.*, 1982; Lo Gullo and Salleo, 1988; Goldstein *et al.*, 1998; Mencuccini *et al.*, 2000). That instantaneous g_s can be non-uniform over a leaf is a well-known fact which has been known for some time, and the mere existence of heterogeneity found for g_s in *A. macrophylla* is therefore not surprising. There are different kinds of spatial heterogeneity of stomatal aperture or g_s that have been reported so far, reaching from the microscale, i.e. from small groups of stomata (stomatal patchiness), to whole leaf regions on the macroscale (Beyschlag and Pfanz, 1990; Terashima, 1992; Pospíšilová and Šantrůček, 1994; Weyers and Lawson, 1997; Lawson and Weyers, 1999; Mott and Buckley, 2000).

Particularly remarkable for *A. macrophylla* are the substantial zonal differences in the diurnal courses of g_s over its large leaves that produce a co-ordinated spatial–temporal pattern. Some recent reports of macroscopic and temporal heterogeneity of g_s or stomatal aperture over leaf laminae exist for *C. communis* (Smith *et al.*, 1989), *Phaseolus vulgaris* (Lawson and Weyers, 1999), *Tradescantia virginiana* (Nejad

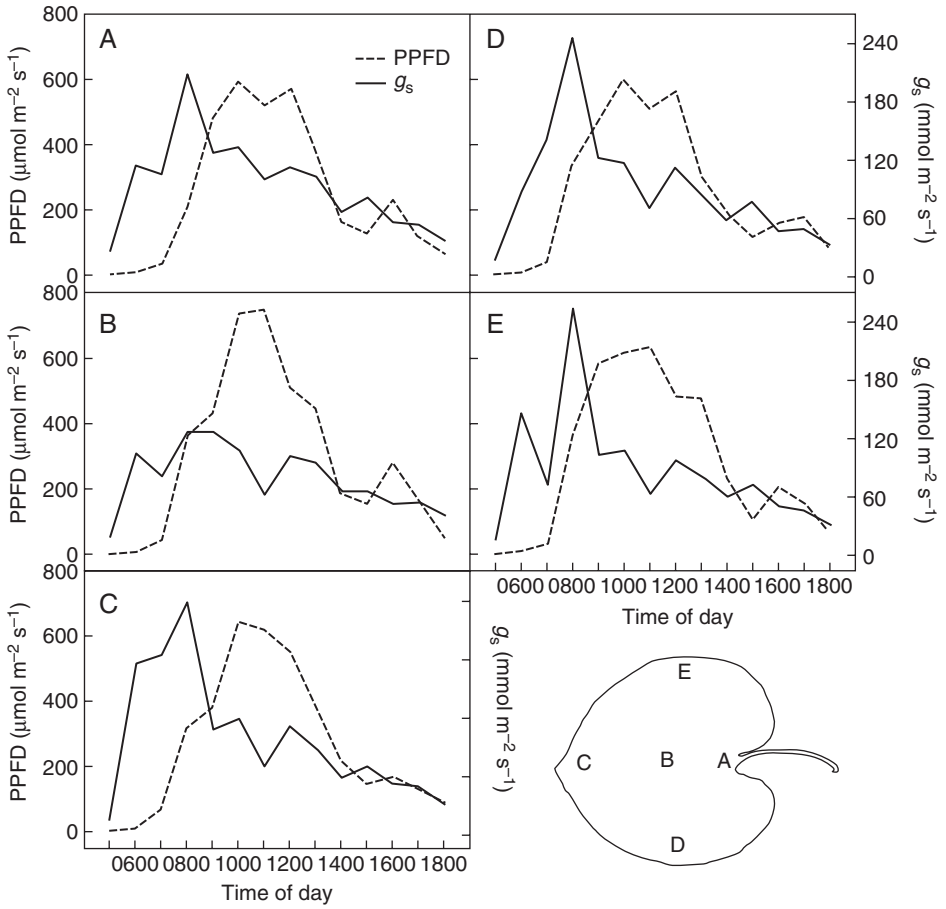

FIG. 6. Course of mean hourly daily PPFD that was received by the leaf zones 1–5, plotted together with mean hourly g_s at these zones. (A) Leaf zone 1. (B) Leaf zone 2. (C) Leaf zone 3. (D) Leaf zone 4. (E) Leaf zone 5.

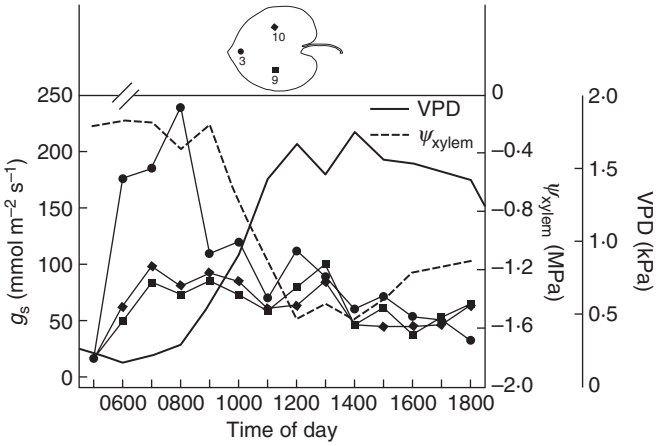

FIG. 7. Course of mean hourly daily VPD and ψ_{xylem} of the stem, plotted together with mean hourly g_s at the leaf zones 3, 9 and 10, as indicated in the inset illustration.

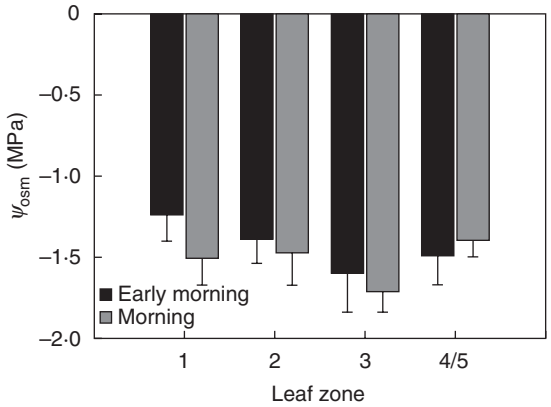

FIG. 8. Mean ψ_{osm} of leaf zones 1–3 and 4/5 (leaf margin) in the early morning (EM, 0500–0800 h) and morning (M, from after 0800 h to 1100 h). The error bars represent the s.e.

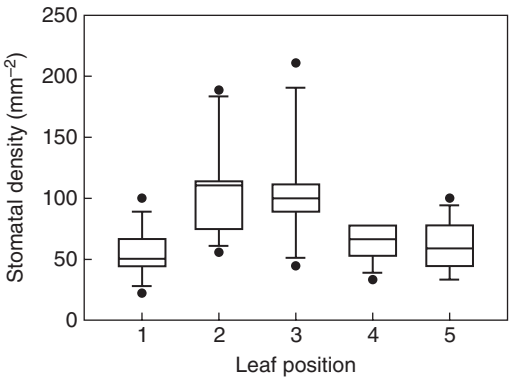

FIG. 9. Stomatal density at leaf zones 1–5. The boxes span the 50 % interquartile, and the median is indicated by the horizontal line within the boxes. The error bars mark the highest and lowest value. Outliers are indicated by circles.

et al., 2006) and *N. tabacum* (Nardini *et al.*, 2008). In *C. communis*, stomatal aperture peaks during noon, with the largest aperture in the leaf centre and a gradually decreasing

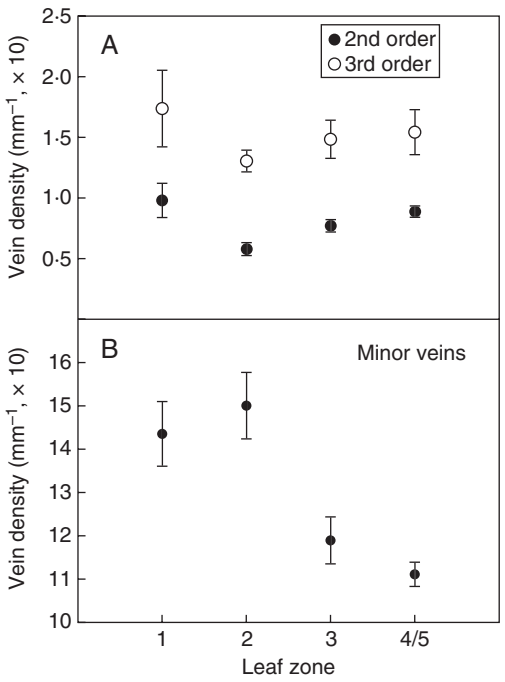

FIG. 10. Vein density at leaf zones 1–3 and 4/5 (leaf margin). (A) Density of second and third order veins. (B) Density of minor veins. The error bars represent the s.e.

TABLE 2. *Length (d) of the long and short axes of the elliptically shaped cross-sections of the conduits inside the major leaf vein in* A. macrophylla *and the number of conduits inside the vein at three different leaf zones (base, centre and tip). The potential hydraulic conductivity of the vein (K_h), approximated by using the conduit dimensions, is also shown*

Leaf zone	$d_{Long\ axis}$ (μm)	$d_{Short\ axis}$ (μm)	$n_{conduits}$	K_h (m^4 MPa^{-1} s^{-1})
1 (base)	30·1 ± 8·3	19·9 ± 6·6	53 ± 8·3	4·31 × 10^{-10}
2 (centre)	28·4 ± 2·9	20·1 ± 7·3	27 ± 2·9	1·96 × 10^{-10}
3 (tip)	11·6 ± 2·5	8·2 ± 2·2	10 ± 3·5	1·53 × 10^{-12}

aperture towards the leaf margins (Smith *et al.*, 1989). In *T. virginiana*, depending on the growth conditions, stomata located at the margin of the leaves tended to close more readily after leaf excision than those located at the leaf centre (Nejad *et al.*, 2006). To our knowledge, the present study is the first one to document data of spatial–temporal patterns in g_s across leaves over whole vegetation periods under natural conditions. The different diurnal patterns in g_s at the considered leaf zones, shown in Figs 5–7, indicate a trend of zone-specific stomatal behaviour, with the leaf tip showing high g_s preferably during the early morning. Quite striking in this respect is the symmetric nature of this spatial–temporal pattern: the right and left leaf zones, for example, express a synchronous pattern. On the whole, the marginal regions and tip appear to show similar diurnal patterns and amplitude of $g_{s,zonal}$.

It is unlikely that the observed differences in diurnal patterns of g_s at the various leaf zones of *A. macrophylla* are

caused by stomatal responses to leaf microclimate or weather conditions since different leaves were monitored over two vegetation periods. The growing site was well watered during the whole observation period by regular precipitation events, also demonstrated by ψ_{soil} which seldom dropped below −0·1 MPa. Various causes are suggested to lead to macroscopic differences in stomatal aperture or g_s. Local differences in SD and stomatal size are known to occur and may contribute to g_s differences over a leaf (Poole *et al.*, 1996; Weyers and Lawson, 1997). The results of local SD in *A. macrophylla* revealed higher values at the leaf centre and tip, compared with the margins and base. Since diurnal variations of g_s are not directly consistent with these SD differences, it is unlikely that the spatial and temporal patterns of g_s in *A. macrophylla* were caused by stomatal frequency distribution.

Microclimatic differences over a leaf were suggested as another factor that is able to generate local differences in g_s. Crucial for local microclimatic conditions at a certain leaf zone is – with all other factors being equal – the boundary layer thickness that tends to be higher in the central leaf region compared with the leaf margins and tip (Schuepp, 1993; Weyers and Lawson, 1997). An increase in boundary layer thickness towards the leaf centre is expected particularly for large and whole leaves, with a substantial parallel decrease in mass and heat transfer (Vogel, 1968; Grace *et al.*, 1980; Roth-Nebelsick, 2001). Intuitively, it appears therefore to be beneficial for a large leaf to allow higher g_s in the leaf centre where the boundary layer tends to be thicker and the risk of heat stress higher than at the margins or tip. The observation of higher g_s values in the central part of *C. communis* leaves compared with the margins, as reported by Smith *et al.* (1989), would match this assumption.

The results of the present study, that shows for *A. macrophylla* higher g_s at the tip and leaf margins compared with the leaf centre, contradict this idea. The possibility exists that g_s may have been systematically altered in the centre of the leaves during measurements due to disturbance of a thick central boundary layer by the measurement cup. In this case, however, central g_s values would be expected to be more or less homogeneously affected, and diurnal patterns at the respective zones would have become less obvious. However, g_s values at different zones in the middle area of the leaf (leaf zones 2, 7, 10 and 12) show substantial and systematic differences with respect to diurnal patterns. There are also distinct differences in the patterns at the leaf margins and the tip, both of which should show similarly thin boundary layers. It should also be noted that even moderate wind velocities cause more complex patterns of boundary layer thickness in which differences between the leaf margins and centre are blurred (Wigley and Clark, 1974). The climate data recorded during our measurements indicate that some wind was often present at the considered site, usually with velocities around 1 m s^{-1}.

Leaf zonal g_s *and water supply*

The natural habitat of *A. macrophylla*, often dissected uplands and rocky slopes within forests of the Cumberland and Blue Ridge mountains in the eastern USA, corresponds to the obviously quite high water demand of this species that is also indicated by its large and thin leaves. Leaf size is a trait linked to climate, with large-leaved species tending to prefer moist and/or shady habitats (Givnish, 1987; Peppe *et al.*, 2011). Since leaf venation systems can offer substantial resistance to flow (Cochard *et al.*, 2004), a steep water potential gradient may develop if homogeneous evaporation occurs over the whole lamina of a large leaf with unsustainably high negative water potentials particularly at the leaf margins or tip.

In *N. tabacum*, which has large leaves with a size and shape similar to those of *A. macrophylla*, both g_s and venation density were found to be higher at the leaf tip than at the leaf base (Nardini *et al.*, 2008). Since no diurnal pattern of g_s was provided for *N. tabacum*, it is not clear whether g_s at the leaf tip was constantly higher than at the base. If so, then it is possible that high apical g_s in *N. tabacum* is supported by the higher venation density at this leaf zone, because K_{leaf} is positively correlated with venation density. In *A. macrophylla*, however, no higher venation density could be found at the leaf margins or tip. On the contrary, minor venation density was lower at the tip and margin in *A. macrophylla* leaves as compared with the other leaf zones considered. Also, local K_{leaf} in *A. macrophylla* probably decreases further with increasing distance from the petiole, since the number and size of the major vein conduits decreases in the same direction. Although K_{vein}, the hydraulic conductivity of a leaf vein, depends on various factors, conduit size and number will dictate maximum K_{vein}.

Hydraulic supply of a leaf, expressed by leaf hydraulic conductance K_{leaf}, or its reverse, resistance, is in fact linked to gas exchange regulation (Sack and Holbrook, 2006; Guyot *et al.*, 2012). There is evidence that the venation of large leaves is more prone to cavitation, compared with smaller leaves (Scoffoni *et al.*, 2011). In a study on gas exchange of different cultivars of *P. vulgaris*, it was found that g_s was negatively correlated with typical leaf size (Mencuccini and Comstock, 1999), supporting the idea that leaf water transport represents a bottleneck for gas exchange particularly in large leaves. The spatial–temporal pattern of g_s expressed by *A. macrophylla* appears to represent a quite appropriate strategy to prevent water stress and subsequent vein embolism in peripheral regions of large leaves. The leaf tip, showing the greatest distance to the petiole, performs its highest gas exchange rate in the early morning, starting with dawn, when the VPD is still low to moderate. The leaf margins follow thereafter. All marginal regions including the tip then decrease their g_s well before ψ_{xylem} plunges after they have exploited the morning as a time slot of favourable conditions for gas exchange. In fact, the pre-noon decrease of g_s in the tip and margins leads to a short recovery of ψ_{xylem} (Fig. 7). The values of g_s in all other regions tend to moderate to low values over the whole day that decline more or less gradually towards the evening. The low variability in ψ_{osm} found for the various leaf zones might also indicate that the observed g_s patterns prevent turgor loss.

Despite this gradual decline in mean g_s, the transpirational load upon the xylem increases, driven by the VPD increase that sets in during the morning. Mean daily minimum ψ_{xylem} in *A. macrophylla* during the growing season is similar to typical values found for mesophytic woody plants (Larcher,

2003), and it may be assumed that beyond this value risk of embolism will rise. Furthermore, vulnerability to embolism can be higher in the leaf veins than in the stem (Salleo *et al.*, 2001), and a close co-ordination between leaf conductance and g_s was repeatedly reported (Brodribb *et al.*, 2003; Sack and Holbrook, 2006). Therefore, the tendency for stomatal limitation and leaf zonal patterns of g_s in *A. macrophylla* appears to be necessary to prevent ψ_{xylem} from entering a regime of high cavitation risk, thereby avoiding embolism, a crucial prerequisite for maximizing carbon gain.

Conclusions

The diurnal course of gas exchange regulation in *A. macrophylla* leaves depends on the leaf zone. Positional co-ordination of gas exchange is commonly found for the different insertion heights within a plant (Larcher, 2003; Sellin and Kupper, 2005). These intercanopy gradients reflect not only differences in microclimate but also local water deficits and/or hydraulic constraints. The entire plant water system with its local differentiations is integrated by stomatal function modulating supply and demand (Sellin and Kupper, 2005). The spatial–temporal trends in g_s over *A. macrophylla* leaves may indicate that the inherent hydraulic differentiations found for whole plants can be repeated on a smaller scale in large leaves. If this finding turned out to be a general strategy of gas exchange regulation in large leaves, then other leaf traits may be involved, such as leaf venation architecture. *Aristolochia macrophylla* leaves show a palmate venation that may convey a particularly appropriate hydraulic system for independently regulated units of a whole leaf. There is in fact evidence that leaves showing palmate venation systems, often of the macrophyll class, are quite unaffected by major vein damage (Sack *et al.*, 2008). Possibly, this venation type facilitates hydraulic and gas exchange partitioning of large leaves.

SUPPLEMENTARY DATA

Supplementary data are available online at www.aob.oxfordjournals.org and consist of the following. Figure S1: image of the study plant. Figure S2: illustration of the lamina fields that were considered for venation density. Figure S3: raw data of hourly g_s for all leaf lamina zones. Table S1: results of the statistical tests of zonal differences in g_s.

ACKNOWLEDGEMENTS

We wish to thank the Botanical Garden of the University of Tübingen for providing access to the plant and for helpful support. We also thank Hartmut Schulz, University of Tübingen, for assisting with the SEM studies, and Stephan Ebner, Tübingen for programming the Interpolation Tool within MATLAB. We gratefully acknowledge James Nebelsick (University of Tübingen) for critically reading the English manuscript. This manuscript greatly benefitted from the comments of two anonymous reviewers and the Handling Editor, Jiří Šantrůček. This work was supported by the German Federal Ministry of Education and Research (Project 'Fibre-based transport of liquids', no. 01RB0713A by a grant to A.R.-N., within the programme 'BIONA').

LITERATURE CITED

Ball JT, Woodrow IE, Berry JA. 1987. A model predicting stomatal conductance and its contribution to the control of photosynthesis under different environmental conditions. *Progress in Photosynthesis Research* **4**: 221–224.

Berninger F, Mäkela A, Hari P. 1996. Optimal control of gas exchange during drought: empirical evidence. *Annals of Botany* **77**: 469–476.

Beyschlag W, Pfanz H. 1990. A fast method to detect the occurrence of non-homogeneous distribution of stomatal aperture in heterobaric plant leaves. Experiments with *Arbutus unedo* L. during the diurnal course. *Oecologia* **82**: 52–55.

Brodribb TJ, Holbrook NM, Edwards EJ, Gutiérrez MV. 2003. Relations between stomatal closure, leaf turgor and xylem vulnerability in eight tropical dry forest trees. *Plant, Cell and Environment* **26**: 443–450.

Bruus H. 2008. *Theoretical microfluidics*. New York: Oxford University Press.

Buckley TN. 2005. The control of stomata by water balance. *New Phytologist* **168**: 275–292.

Cochard H, Nardini A, Coll L. 2004. Hydraulic architecture of leaf blades: where is the main resistance? *Plant, Cell and Environment* **27**: 1257–1267.

Collatz GJ, Ball MC, Grivet C, Berry JA. 1991. Physological and environmental regulation of stomatal conductance, photosynthesis, and transpiration: a model that includes a laminar boundary layer. *Agricultural and Forest Meterology* **54**: 107–136.

Cowan IR, Farquhar GD. 1977. Stomatal function in relation to leaf metabolism and environment. *Symposium of the Society for Experimental Biology* **31**: 471–505.

Damour G, Simonneau T, Cochard H, Urban L. 2010. An overview of models of stomatal conductance at the leaf level. *Plant, Cell and Environment* **33**: 1419–1438.

Dewar RC. 2002. The Ball–Berry–Leuning and Tardieu–Davies stomatal models: synthesis and extension within a spatially aggregated picture of guard cell function. *Plant, Cell and Environment* **25**: 1383–1398.

Dixon MA, Tyree MT. 1984. A new stem hygrometer, corrected for temperature gradients and calibrated against the pressure bomb. *Plant, Cell and Environment* **7**: 693–697.

Ellis B, Daly DC, Hickey LJ, *et al.* 2009. *Manual of leaf architecture*. Ithaca: The New York Botanical Garden Press.

Givnish TJ. 1987. Comparative studies of leaf form: assessing the relative roles of selective pressures and phylogenetic constraints. *New Phytologist* **106**: 131–160.

Goldstein G, Andrade JL, Meinzer FC, *et al.* 1998. Stem water storage and diurnal patterns of water use in tropical forest canopy trees. *Plant, Cell and Environment* **21**: 397–406.

Grace J, Fasehun FE, Dixon M. 1980. Boundary layer conductance of the leaves of some tropical timber trees. *Plant, Cell and Environment* **3**: 443–450.

Guyot G, Scoffoni C, Sack L. 2012. Combined impacts of irradiance and dehydration on leaf hydraulic conductance: insights into vulnerability and stomatal control. *Plant, Cell and Environment* **35**: 857–871.

Hammer Ø, Harper DAT, Ryan PD. 2001. PAST: paleontological statistics software package for education and data analysis. *Palaeontologia Electronica* **4**.

Jones HG. 1992. *Plants and microclimate*. Cambridge: Cambridge University Press.

Kaiser H. 2009. The relation between stomatal aperture and gas exchange under consideration of pore geometry and diffusional resistance in the mesophyll. *Plant, Cell and Environment* **32**: 1091–1098.

Katul G, Manzoni S, Palmroth S, Oren R. 2010. A stomatal optimization theory to describe the effects of atmospheric CO_2 on leaf photosynthesis and transpiration. *Annals of Botany* **105**: 431–442.

Lang ARG. 1967. Osmotic coefficients and water potentials of sodium chloride solutions from 0 to 40 °C. *Australian Journal of Chemistry* **20**: 2017–2023.

Larcher W. 2003. *Physiological plant ecology*, 4th edn. Cambridge: Cambridge University Press.

Lawson T, Weyers J. 1999. Spatial and temporal variation in gas exchange over the lower surface of *Phaseolus vulgaris* L. primary leaves. *Journal of Experimental Botany* **50**: 1381–1391.

Leuning R. 1995. A critical appraisal of a combined stomatal–photosynthesis model for C_3 plants. *Plant, Cell and Environment* **18**: 339–355.

Leyton L. 1975. *Fluid behaviour in biological systems*. Oxford: Clarendon Press.

Lo Gullo MA, Salleo S. 1988. Different strategies of drought resistance in three mediterranean sclerophyllous trees growing in the same environmental conditions. *New Phytologist* **108**: 267–276.

Lösch R, Tenhunen JD, Pereira JS, Lange OL. 1982. Diurnal courses of stomatal resistance and transpiration of wild and cultivated Mediterranean perennials at the end of the summer dry season in Portugal. *Flora* **172**: 138–160.

Mencuccini M, Comstock J. 1999. Variability in hydraulic architecture and gas exchange of common bean (*Phaseolus vulgaris*) cultivars under well-watered conditions: interactions with leaf size. *Australian Journal of Plant Physiology* **26**: 115–124.

Mencuccini M, Mambelli S, Comstock J. 2000. Stomatal responsiveness to leaf water status in common bean (*Phaseolus vulgaris*) is a function of time of day. *Plant, Cell and Environment* **23**: 1109–1118.

Mott KA, Buckley TN. 2000. Patchy stomatal conductance: emergent collective behaviour of stomata. *Trends in Plant Science* **5**: 258–262.

Nardini A, Gortan E, Ramani M, Salleo S. 2008. Heterogeneity of gas exchange rates over the leaf surface in tobacco: an effect of hydraulic architecture? *Plant, Cell and Environment* **31**: 804–812.

Nejad AR, Harbinson J, van Meeteren U. 2006. Dynamics of spatial heterogeneity of stomatal closure in *Tradescantia virginiana* altered by growth at high relative air humidity. *Journal of Experimental Botany* **57**: 3669–3678.

Peppe DJ, Royer DL, Cariglino B, *et al*. 2011. Sensitivity of leaf size and shape to climate: global patterns and paleoclimatic applications. *New Phytologist* **190**: 724–739.

Poole I, Kürschner WM. 1999. Stomatal density and index: the practice. In: Jones TP, Rowe NP. eds. *Fossil plants and spores: modern techniques.* London: The Geological Society, 257–260.

Poole I, Leyers JDB, Lawson T, Raven JA. 1996. Variations in stomatal density and index: implications for paleoclimatic reconstructions. *Plant, Cell and Environment* **19**: 705–712.

Pospíšilová J, Šantrůček J. 1994. Stomatal patchiness. *Biologia Plantarum* **36**: 481–510.

Rasband WS. 1997–2012. *ImageJ*. http://imagej.nih.gov/ij/. (accessed 10 November, 2012).

Roth-Nebelsick A. 2001. Computer-based analysis of steady-state and transient heat transfer of small-sized leaves by free and mixed convection. *Plant, Cell and Environment* **24**: 631–640.

Roth-Nebelsick A, Uhl D, Mosbrugger V, Kerp H. 2001. Evolution and function of leaf venation architecture: a review. *Annals of Botany* **87**: 553–566.

Sack L, Holbrook NM. 2006. Leaf hydraulics. *Annual Review of Plant Biology* **57**: 361–381.

Sack L, Dietrich EM, Streeter CM, Sánchez-Gómez D, Holbrook NM. 2008. Leaf palmate venation and vascular redundancy confer tolerance of hydraulic disruption. *Proceedings of the National Academy of Sciences, USA* **105**: 1567–1572.

Salleo S, LoGullo MA, Raimondo F, Nardini A. 2001. Vulnerability to cavitation of leaf minor veins: any impact on leaf gas exchange? *Plant, Cell and Environment* **24**: 851–859.

Schuepp PH. 1993. Tansley Review No. 59. Leaf boundary layers. *New Phytologist* **125**: 477–507.

Scoffoni C, Rawls M, McKown A, Cochard H, Sack L. 2011. Decline of leaf hydraulic conductance with dehydration: relationship to leaf size and venation architecture. *Plant Physiology* **156**: 832–843.

Sellin A, Kupper P. 2005. Effects of light availability versus hydraulic constraints on stomatal responses within a crown of silver birch. *Oecologia* **142**: 388–397.

Smith S, Weyers JDB, Berry WG. 1989. Variation in stomatal characteristics over the lower surface of *Commelina communis* leaves. *Plant, Cell and Environment* **12**: 653–659.

Sperry JS, Hacke UG, Oren R, Comstock JP. 2002. Water deficits and hydraulic limits to leaf water supply. *Plant, Cell and Environment* **25**: 251–263.

Terashima I. 1992. Anatomy of non-uniform leaf photosynthesis. *Photosynthesis Research* **31**: 195–212.

Vogel S. 1968. 'Sun leaves' and 'shade leaves': differences in convective heat dissipation. *Ecology* **49**: 1203–1204.

Vogt UK. 2001. Hydraulic vulnerability, vessel refilling, and seasonal courses of stem water potential of *Sorbus aucuparia* L. and *Sambucus nigra* L. *Journal of Experimental Botany* **52**: 1527–1536.

Weyers JDB, Lawson T. 1997. Heterogeneity in stomatal characteristics. *Advances in Botanical Research* **26**: 317–352.

Wigley G, Clark JA. 1974. Heat transport coefficients for constant energy flux models of broad leaves. *Boundary-Layer Meteorology* **7**: 139–150.

Wong SC, Cowan IR, Farquhar GD. 1979. Stomatal conductance correlates with photosynthetic capacity. *Nature* **282**: 424–426.